HHS Public Access

Author manuscript

Breast Cancer Res Treat. Author manuscript; available in PMC 2020 June 01.

Published in final edited form as:

Breast Cancer Res Treat. 2019 June ; 175(2): 353–368. doi:10.1007/s10549-018-05108-5.

ERα upregulates the expression of long non-coding RNA *LINC00472* which suppresses the phosphorylation of NF-κB in breast cancer

Zhanwei Wang[1], **Dionyssios Katsaros**[2], **Nicoletta Biglia**[3], **Yi Shen**[1], **Lenora Loo**[1], **Xiao Yu**[4], **Hongyan Lin**[4], **Yuanyuan Fu**[1,5], **Wen-Ming Chu**[1], **Peiwen Fei**[1], **Yan Ni**[1], **Wei Jia**[1], **Xiaobei Deng**[4], **Biyun Qian**[4,*], and **Herbert Yu**[1,*]

[1]University of Hawaii Cancer Center, Honolulu, Hawaii

[2]Department of Surgical Sciences, Gynecology, AOU Città della Salute, University of Torino, Turin, Italy

[3]Department of Surgical Sciences, Division of Obstetrics and Gynecology, University of Torino School of Medicine, Mauriziano Hospital, Turin, Italy

[4]Shanghai Jiao Tong University School of Medicine, Shanghai, China

[5]Department of Molecular Biosciences & Bioengineering, University of Hawaii at Manoa, Honolulu, Hawaii

Abstract

Low expression of long intergenic non-coding RNA *LINC00472* in breast cancer is associated with aggressive tumors and unfavorable disease outcomes. To study the mechanisms underlying these associations, we investigated the molecular targets and regulation of *LINC00472* in breast cancer cells, and analyzed relevant molecular features in relation to patient survival. Gene expression profiles of breast cancer cells overexpressing *LINC00472* were analyzed for its regulatory pathways and downstream targets. Effects of *LINC00472* overexpression on cell behaviors were evaluated *in vitro* and *in vivo*. Meta-analysis was performed using online datasets and our own study. Analysis of *LINC00472* transcriptome revealed ERα upregulation of *LINC00472* expression, and an ERα-binding site in the *LINC00472* promoter was identified. Evaluation of *LINC00472* overexpression also indicated a possible link between *LINC00472* and NF-κB. Cell experiments confirmed that *LINC00472* suppressed the phosphorylation of p65 and IκBα through binding to IKKβ, inhibiting its phosphorylation. High *LINC00472* expression

*Corresponding authors: Herbert Yu, MD, PhD, University of Hawaii Cancer Center, 701 Ilalo Street, Honolulu, HI 96813, hyu@cc.hawaii.edu, Biyun Qian, MD, PhD, Hongqiao International Institute of Medicine, Shanghai Tongren Hospital and Faculty of Public Health, Shanghai Jiao Tong University School of Medicine, 227 South Chongqing Road, Shanghai 200025, China, qianbiyun@shsmu.edu.cn.

Conflict of interest: All authors declare no conflict of interest.

Ethical approval for animal use: All applicable international, national and/or institutional guidelines for the care and use of animals were followed.

Ethical approval for human study: All study procedures involving human participants were in accordance with the ethical standards of the institutional and/or national research committee with the 1964 Helsinki declaration and its later amendments or comparable ethical standards.

Informed consent: Informed consent was obtained from all individual participants included in the study.

inhibited tumor growth both *in vitro* and *in vivo* and suppressed aggressive tumor cell behaviors *in vitro*. Suppressing *LINC00472* expression in ER-positive tumor cells increased cell aggressive behaviors. Tamoxifen treatment of ER-positive cells inhibited ERα and *LINC00472* expression and increased p65 and IκBα phosphorylation. Meta-analysis showed that *LINC00472* expression were higher in ER-positive than ER-negative tumors and that high expression was associated with better disease outcomes in ER-positive patients. The study demonstrates that ERα upregulates *LINC00472* which suppresses the phosphorylation of NF-κB, and suggests that endocrine treatment may lower *LINC00472* and increase NF-κB activities, leading to tumor progression and disease recurrence.

Keywords

LINC00472; breast cancer; ERα; NF-κB; endocrine resistance; lncRNA; prognosis

Introduction

Status of estrogen receptor (ER) in breast cancer is a valuable biomarker for prediction of disease prognosis and patient response to endocrine therapy. Most patients with ER-positive breast cancer are responsive to tamoxifen treatment with favorable prognosis, but some of them develop endocrine resistance, which leads to disease recurrence and tumor metastasis (1-3). Several theories have been proposed to explain the mechanisms of endocrine resistance in breast cancer, one of which is the reciprocal suppression between two important cell signaling pathways, ERα and NF-κB (4). Evidence suggests that ER may suppress the activity of NF-κB and that endocrine therapy blocks the action of ER, which reduces NF-κB suppression by ER. NF-κB, a transcription factor regulating immunity, inflammation and many important cell functions, is known to play a crucial role in tumor progression and metastasis (5-9).

Long non-coding RNAs (lncRNAs) have important biological functions (10), and are significantly involved in the development and progression of malignant tumors (11, 12). We found a long intergenic non-coding RNA, *LINC00472*, in breast cancer, low expression of which was associated with aggressive tumor features and unfavorable disease outcomes (13, 14). Our experiments also showed that overexpression of *LINC00472* in breast cancer cells could suppress cell proliferation and migration. Why *LINC00472* had tumor suppressive effects on breast cancer was unknown. To elucidate the function and regulation of *LINC00472* in breast cancer and explore its clinical implications, we conducted experiments on cell lines and xenograft mouse models, and analyzed clinical datasets. Our investigation revealed that ERα upregulated *LINC00472* expression which suppressed the phosphorylation of NF-κB, and that tamoxifen treatment could reduce *LINC00472* expression which led to increases in NF-κB phosphorylation. Low expression of *LINC00472* was associated with ER-negative breast cancer and unfavorable survival outcomes.

Methods

Cell culture

Breast cancer cell lines, MCF-7, T47D, MDA-MB-231 (MB231) and Hs578T, were obtained as part of the NCI-60 DTP Human Tumor Cell Screening Panel. SKBR3 (ATCC ® HTB-30™), ZR-75-1(ATCC ® CRL-1500™) and 293T (ATCC ® CRL-3216™) cells were purchased from the American Type Culture Collection. Human mammary epithelial cells (H-6035) were purchased from Cell Biologics, Inc. Cells were cultured according to the manufacturer's instruction, and no ethics approval was required for the use of these cell lines.

Plasmid transfection

A *LINC00472* transcript (2933 bp, NR_026807.1) was assembled and inserted in a lentiviral vector, pCDH-EF1-MCS-pA-PGK-copGFP-T2A-Puro (pCDH), as previously described (13). The sequence of the insert has been confirmed by sequencing. MB231 and Hs578T cells were transfected with the *LINC00472* plasmid or an empty plasmid (pCDH vector only) using the Lipofectamine 3000 reagent (Thermo Fisher Scientific) following the manufacturer's protocol. Cells with stable expression of *LINC00472* were selected through puromycin screening (Thermo Fisher Scientific). To maintain stably transfected cells, puromycin was added into culture medium, and the puromycin-containing culture medium was replaced every 3 days. A single cell clone was also generated from the stable cell pool through the limiting dilution cloning. Plasmids (pCMV-ESR1) with and without the full-length of human *ESR1* (NM_000125, #RC213277) and (pCMV-vector, #PS100001), respectively, were purchased from Origene Technologies, and the plasmids were transfected into the 293T cells and breast cancer cell lines using the Lipofectamine 3000 reagent (Themo Fisher Scientific).

Cell proliferation, migration, and invasion

Cell proliferation, migration and invasion were analyzed as previously described (15). Briefly, for cell proliferation, we seeded the cells onto 96-well plates at 3×10^3 cells per well. After 2 hours of incubation with the WST-1 cell proliferation reagent (Roche Diagnostics GmbH), cell concentrations were measured at 0, 24, 48 and 72 hours of culture with Optical Density (OD) at 450 nm wavelength using a microplate spectrophotometer (Biotek Synergy 2). Cell migration and invasion assays were performed using the Costar Transwell permeable polycarbonate supports (8.0 μm pores) in 24-well plates (Corning Inc.). Cells at a concentration of 1×10^4 per well were seeded onto the upper chambers of the Transwell permeable supports coated with 1 mg/ml growth factor-reduced Matrigel matrix for invasion assay and without the Matrigel coating for migration assay (BD Pharmingen). The lower chambers were filled with 600 μl complete culture medium. Cells migrating to the lower chambers were stained with HEME 3 Solution (Fisher Diagnostics) after 36 hours of incubation. All the assay results were measured in triplicate, and each assay was repeated 3 times.

Colony formation assay

Cells at a concentration of 1×10^3 per well were seeded on 0.3% agarose overlaid onto solidified 0.6% agarose in RPMI1640 with 10% FBS in a 6-well plate. Culture medium (200 μl) containing puromycin was added in each well every three days. After 5 weeks, colonies were counted in 5 selected fields from 3 representative wells using the Bid-Rad colony counter. The assay was repeated 3 times.

Flow cytometry analysis of cell cycle

Cells were first cultured in serum-free medium for 24 hours, followed by replacing it with a medium containing 10% FBS. These cells were harvested after 48 hours of incubation and PBS washing twice, and were fixed in 70% ice-cold ethanol and stained with propidium iodide (BD Biosciences) at a concentration of 1×10^6. Cell population data in different cell cycles were collected using the BD Accuri C6 flow cytometer (BD Biosciences) and analyzed with the FlowJo software. The analysis was performed in triplicate for each experiment, and the experiment was repeated 3 times.

Tumor xenograft model

Seven 5-week old BALB/c female nude mice, SPF grade, were purchased from Shanghai SLAC Laboratory Animal Co., Ltd. for tumor xenograft experiment. The mice were injected with 100 μl of 5×10^6 MB231 cells (50 μl cell solution mixed with 50 μl Matrigel), and the injections were made in the inguinal mammary fat pad with mock cells on the right and *LINC00472* overexpression cells on the left. The mice were monitored for 25 days after injection, and body weight and tumor size were measured every 2-3 days after the first two weeks of injection. Animal procedures were performed according to a study protocol that was approved by the university's Animal Care and Use Committee.

RNA extraction and LINC00472 measurement

Total RNA were extracted from fresh-frozen tumor samples, animal models, and cultured cells using the Allprep DNA/RNA kit (Qiagen). RNA samples were reverse-transcribed (RT) using the cDNA Reverse Transcription kit (LifeTech), and the cDNA samples were analyzed for *LINC00472* expression with quantitative PCR (qPCR) described elsewhere (13).

RNA immunoprecipitation (RIP)

Magna RIP RNA-Binding Protein Immunoprecipitation kit (Millipore) was used for RIP analysis. Antibodies against IKKα (#2682S) and IKKβ (#8943S) were purchased from Cell Signaling Technology. Rabbit IgG antibody (#12-370 from EMD Millipore) was used as control. The RIP assay was performed according to the manufacturer's instructions. In brief, magnetic beads were mixed with cell lysates and antibodies of interest (anti-IKKα, anti-IKKβ, or IgG), and the mixtures were incubated with gentle rotation at room temperature for 4 hours. After incubation, beads were isolated by centrifugation and washed with RIP buffer for 3 times. The beads were re-suspended and divided into two portions, one for western blot analysis after proteins were denatured by heat and one for RNA analysis after co-precipitated RNAs were isolated from the beads according to the protocol. The extracted RNAs were analyzed for *LINC00472* with qRT-PCR.

Western blot analysis

Cell lysates were prepared in a lysis buffer purchased from Roche. The lysates containing 40-60 μg proteins were analyzed with SDS-PAGE under a denaturing condition and the resulting gels were transferred to polyvinylidene difluoride (PVDF) membranes (Millipore). The membranes were blocked with 5% non-fat milk for 45 minutes, and then incubated with a primary antibody followed by a secondary antibody. The signals were detected by an enhanced chemiluminescence system (ECL) following the manufacturer's manual (Pierce). Antibodies used for western blot included anti-Phospho-NF-κB p65 (Ser536) (#3033), anti-NF-κB p65 (#8242), anti-Phospho-IκBα (Ser32) (#2895), anti-IκBα (#9242), anti-IKKα (#2682S), anti-IKKβ (#8943S), anti-ERα (#8644), all of which purchased from Cell Signaling Technology, anti-phospho-IKKβ (ab53694) from Abcam, and antiβ-actin (A2228) from Sigma-Aldrich.

siRNA knockdown

Breast cancer cells and human mammary epithelial cells were transfected with Lincode Human *LINC00472* (79940) siRNA-SMART pool (D-001320-10-05) or Lincode Non-targeting Pool (D-001320-10-05), negative control from Dharmacon, following the manufacturer's protocol for Lipofectamine RNAiMAX (Thermo Fisher Scientific). The method of transfection was described elsewhere (15). Cell lysates were prepared for analysis after 36 hours of incubation of the transfected cells.

Luciferase reporter assay

The pGL4.27 [luc2P/minP/Hygro] vector was purchased from Promega. Synthesizing and inserting the wild and mutant *LINC00472* promoter sequences into the pGL4.27 vector to make pGL4.27-linc00472-wt and pGL4.27-linc00472-mut plasmids were completed and verified by GENEWIZ LLC. The 293T cells were first transiently transfected with pCMV-ESR1 using the Lipofectamine 3000 reagent (Themo Fisher Scientific). After 36 hours of incubation, the plasmid of pGL4.27-linc00472-wt or pGL4.27-linc00472-mut, together with the renilla reporter vector, were transfected into the *ERS1*-expressing cells. Renilla and firefly luciferase activities were measured using the Dual-Luciferase kit (Promega). The results were normalized with the renilla reporter for transfection efficiency. Each assay was performed in triplicate.

Chromatin immunoprecipitation (ChIP)-qPCR assay

ChIP assay was performed using a Chromatin Immunoprecipitation (ChIP) Assay kit (EMD Millipore). After 48-hour incubation of the 293T cells transfected with pCMV-ESR1 or pCMV-vector, formaldehyde was added directly into the culture medium at a final concentration of 1% to crosslink histones and DNA. About 200 μl cell lysates were sonicated to shear DNA into lengths between 200 and 1,000 base pairs. Sonicated nuclear fractions were incubated overnight at 4°C with a rabbit polyclonal antibody against ERα (#8644T from Cell Signaling Technology) or a rabbit polyclonal antibody against IgG (#12-370 from EMD Millipore) as a control. After that, 60 μl of Protein A Agarose/Salmon Sperm DNA (50% Slurry) were added for another hour of incubation at 4°C and then the antibody/histone complex were collected. The complex was washed and eluted with a buffer

supplied in the kit. The eluted histone complex was mixed with 20 μl of 5 M NaCl and heated at 65°C for 4 hours to break the histone-DNA crosslink. Then, 10 μl of 0.5 M EDTA, 20 μl of 1 M Tris-HCl, pH 6.5, and 2 μl of 10 mg/ml Proteinase K were added, and the mixtures were incubated for 1 hour at 45°C. DNA in the samples were isolated through phenol/chloroform extraction and ethanol precipitation. *LINC00472* promoter in the samples was quantified by qPCR using the primers: CTTTCCGACACCTGATT (forward) and TAGCCAATTGGGGTCTTTG (reverse).

TNF-α treatment

TNF-α (Sigma-Aldrich), diluted in the culture medium immediately before experiment, was added to cultured cells with a final concentration of 10 ng/ml. The cells were incubated for 24 hours before analysis. DMSO (Sigma-Aldrich) treated cells were used as control. Total RNA and proteins were extracted for analysis of *LINC00472* expression and NF-κB activation.

Tamoxifen treatment

T-47D cells were cultured in the complete culture medium supplemented with 10μM 4-Hydroxytamoxifen (Sigma-Aldrich), and the medium was changed every two days. After two and eight days of culture, cells were collected, and total RNA and proteins were extracted for qRT-PCR analysis of *LINC00472* and *ESR1* and western blot of ERα and NF-κB, respectively.

Analysis of cell metabolome

Cell lysates were prepared following protocols described previously (16-18). Briefly, appropriate weight of homogenizer beads and 50 μl of cold water were added to cell samples for initial extraction. A 270 μl mixture of ethanol and chloroform, 3:1 (v/v), was added to the initial extracts for second extraction. The final extracts were centrifuged at 14,500 rpm for 20 min at 4°C. The supernatants were used for targeted metabolic profiling of 140 lipids with an Acquity ultra-performance liquid-chromatography coupled with a Xevo TQ-S mass spectrometry (UPLC–TQ-MS, Waters Corp.) (17). The same materials were also utilized for untargeted metabolic profiling using an Agilent 7890A gas chromatography with a Leco Pegasus time-of-flight mass spectrometer (GC-TOF-MS, Leco Corp.) (18). The raw UPLC–TQ-MS data files were processed with Target Lynx Application Manager (Waters Corp.) to extract peak area and retention time of each metabolite. The raw GC–TOF-MS data files were processed with Chroma TOF software (v4.22, Leco Corp.) which performed de-noising, peak detection and compound deconvolution. Internal standards and any known artificial peaks, such as peaks caused by noise, column bleed and BSTFA derivatization procedure, were removed from the data set. For UPLC-TQ-MS, metabolite annotation was performed by comparing the accurate mass (*m/z*) and retention time (Rt) of reference standards in our in-house library and the accurate mass of compounds obtained from the web-based resources such as the Human Metabolome Database (http://www.hmdb.ca). For GC-TOF-MS, metabolites were identified by comparing the mass spectral similarity and retention index distance between the samples and standards of our in-house library. A similarity score of more than 70% was selected for identification.

Analysis of cell transcriptome

Total RNA was extracted from cell lines using the method described earlier. The RNA quality was evaluated with absorbance and RNA Integrity Number (RIN) using the NanoDrop 2000 spectrophotometer (Thermo Fisher Scientific) and Agilent 2100 Bioanalyzer System (Agilent Technologies), respectively. Gene expression data were generated using the Affymetrix Human Transcriptome Array 2.0 (Affymetrix). DNA labeling, probe hybridization, and signal scanning were performed by the Genomic Shared Resource at University of Hawaii Cancer Center. Expression intensities were stored as CEL-files which were processed using the robust multi-array average (RMA) algorithm in the Affymetrix Expression Console for inter-chip quantile normalization. Transcriptome Analysis Console (TAC) v3.0 (Affymetrix) was used to identify genes which were differentially expressed between mock and *LINC00472* cells.

Study patients

We enrolled 525 breast cancer patients in a clinical study. These patients were identified from two hospitals affiliated with University of Torino in Turin, Italy, including 348 patients from the University Hospital enrolled between January 1998 and July 1999 and 177 patients from Mauriziano Hospital recruited between October 1996 and August 2012. Patients gave informed consent for research use of clinical information and tumor specimens. The average age of the patients at surgery was 58 years, and the age range was between 23 and 89 years. Information on disease stage, tumor grade, hormone receptor status, follow-up time and survival outcomes was extracted from medical records. The patient data are shown in Supplementary Table 1. The study was approved by the ethic review committees at the University Hospital and Mauriziano Hospital.

Online datasets

Data on *LINC00472* expression in breast cancer were extracted from the NCBI GEO database (https://www.ncbi.nlm.nih.gov/gds). A total of 15 datasets with at least 100 patients in each were identified from the database, of which 13 had relapse-free survival information (GSE19615, GSE42568, GSE1456, GSE53031, GSE7390, GSE11121, GSE22219, GSE3494, GSE21653, GSE4922, GSE31448, GSE2034, GSE25066), and 5 had overall survival data (GSE42568, GSE16446, GSE1458, GSE7390, GSE20685). Of these datasets, 10 and 2, respectively, had information on both survival and ER status. Compared to the datasets used before (13), four more with relapse-free or overall survival information were identified (GSE22219, GSE53031, GSE25066, and GSE16446). We excluded two previous datasets (GSE25065 and GSE25055) because they were subsets of GSE25066. Datasets without survival information or ER status were not included.

Bioinformatics and statistical analysis

Ingenuity Pathway Analysis (IPA) was used to analyze the transcriptomic and metabolomic data in prediction of the biological network associated with *LINC00472* overexpression. Transcripts and metabolites which had 2-fold changes in expression or concentration, respectively, due to *LINC00472* overexpression ($p<0.05$) were included in the IPA. Downstream pathways (or targets) and upstream signals (or transcription factors) predicted

by IPA were considered for further evaluation only when the prediction was made identical in both cell lines. PROMO (http://alggen.lsi.upc.es) was employed with 5% dissimilarity for predicting the binding sites of transcription factors in the *LINC00472* promoter (19).

Values of *LINC00472* expression in our study and from online datasets were log2 transformed, and their differences by ER status were compared using the Student t test. Meta-analysis was performed to evaluate *LINC00472* expression in association with ER status after the expression was dichotomized using the study-specific median as cutoff. For survival analysis, *LINC00472* expression was also dichotomized as described above. Unadjusted hazards ratios (HRs) and 95% confidence interval (CI) for relapse and death were calculated for each dataset. Pooled HR and 95%CI were estimated using the random-effect model (the DerSimonian and Laird method) (20, 21). Comprehensive Meta-Analysis (v2.0, BIOSTAT) was used for meta-analysis. Values shown in cell experiments were means and standard deviations (SD). Two-tailed Student t test was used to compare means between groups. Paired t-test was used to compare paired differences in the same animals. Two-side p value less than 0.05 was considered statistical significance. Statistical Analysis System v9.4 (SAS Institute Inc.) was used for data analysis.

Results

LINC00472 expression in breast cancer cells

LINC00472 expression was analyzed in one human mammary epithelial cells and six breast cancer cell lines, including three sex hormone receptor-positive (MCF-7, T47D, ZR-75-1), two triple-negative (MB231, Hs578T), and one Her2-positive (SKBR3). The expression was quite high in normal cells, but low in all the cell lines, except for T47D which had higher expression than other tumor cells but lower than the normal one (Fig. 1A). To evaluate the effect of *LINC00472* overexpression on aggressive breast cancer cells, we stably transfected MB231 and Hs578T with a *LINC00472*-expressing plasmid. After transfection, *LINC00472* expression was significantly increased in the cell lines, both in pool and a single clone (Fig. 1B).

Suppression of tumor cell aggressive behaviors by LINC00472

LINC00472 overexpression significantly reduced cell proliferation (Fig. 1C) as well as inhibited cell migration (Fig. 1D) and invasion (Fig. 1E). The overexpression cells were less likely to form colonies in soft agar (Fig. 1F), and had fewer cells in G2 phase (Fig. 1G). All the findings were consistent between the two cell lines.

Suppression of tumor growth by LINC00472

A xenograft model was developed by injecting MB231cells into the mammary fat pad of seven BALB/c female nude mice. Tumors from the *LINC00472* overexpression cells grew much smaller (Fig. 2A), with slower tumor growth rate (Fig. 2B) and higher *LINC00472* expression in the tumors (Fig. 2C). Tissue analysis showed less malignant morphology in tumors with *LINC00472* overexpression (left) than those without overexpression (Fig. 2D).

Analysis of LINC00472-related transcription and metabolism

Gene expression profiles of MB231 and Hs578T cells were analyzed with an Affymetrix microarray chip. Comparing the expression data from 8 cell samples (two pools and two single colons in each of the two cell lines), we found 2 up- and 2 down-regulated transcripts shared by all the 8 samples (Fig. 3A), including *LINC00472*, *DXO*, *LINC01061 and MALAT1*, respectively. Upregulated *LINC00472* expression was expected in the cells transfected with a *LINC00472* plasmid. To validate the microarray findings, we performed qRT-PCR analysis on three top transcripts, and the PCR results were consistent with the microarray findings (Fig. 3B). The gene expression profiles related to *LINC00472* overexpression were interrogated by the Ingenuity Pathway Analysis (IPA) for gene-enriched biological network. Fig. 3C shows the top five canonical pathways where significant gene enrichment was observed due to *LINC00472* overexpression. The two cell lines had five different canonical pathways ranked at the top for gene-enrichment, but the TNF-α pathway was suggested by IPA in both cell lines, although it was not included in the top five pathways ranked by the number of genes enriched.

In the analysis of metabolomes, we found 30 metabolites in MB231 and 15 in Hs578T significantly associated with *LINC00472* overexpression. IPA of these metabolites showed that the top five canonical pathways, except tRNA Charging, were different between the cell lines (Fig. 3D). Upregulation of super pathway of methionine degradation was indicated by IPA in both cell lines, although it was not listed in the top five pathways in one cell line (MB231).

Inhibition of NF-kB phosphorylation by LINC00472

Following the IPA prediction, we tested if TNF-α had any influences on *LINC00472* expression in breast cancer cells. Our experiments showed no changes in *LINC00472* expression in relation to TNF-α, but NF-κB phosphorylation, a downstream target of TNF-α, was suppressed by *LINC00472* overexpression. Based on the observation of *LINC00472*-related super pathway of methionine degradation in our metabolomics analysis and possible involvement of NF-κB in the super pathway of methionine degradation reported in the literature (22, 23), we examined the effect of *LINC00472* on NF-κB, and found significant decreases in phosphorylation of IκBα (one of the IκB proteins) and p65 (RelA) when *LINC00472* was overexpressed (Fig. 3E), suggesting NF-κB being a possible target of *LINC00472*. Further analysis of the IκB kinase (IKK) which activates NF-κB, we found that *LINC00472* interacted with IKKβ (Fig. 3F), but not IKKα (Fig. 3G).

Upregulation of LINC00472 by ERα

IPA predicted eight molecules as possible upstream signals for *LINC00472* in both cell lines (Fig. 4A), one of which was *ESR1*, the estrogen receptor alpha (ERα) gene. We also used PROMO to interrogate the promoter sequence of *LINC00472* in search for its transcription factors (TF). The software predicted a region, −591 to −595, as a possible binding site for ERα (Fig. 4B). We performed a luciferase reporter assay to evaluate the interaction between ERα and the *LINC00472* promoter. The assay results showed that after overexpressing *ESR1* in 293T (Fig. 4C), cells transfected with an intact promoter of *LINC00472* had elevated luciferase signals, whereas the cells with a mutant *LINC00472* promoter that did

not contain the ERα binding site had no increase in luciferase activity (Fig. 4D). A ChIP assay further demonstrated that ERα was able to bind to the *LINC00472* promoter (Fig. 4E). Transfecting Hs578T and MB231 with the *ESR1* plasmid (Fig. 4F and 4H) increased *LINC00472* expression in both cells (Fig. 4G and 4I). Cells with overexpressed ERα had reduced phosphorylation of IκBα and p65 (Fig. 4J). Suppressing *L1NC00472* expression by siRNA (Fig. 4K) could increase NF-κB phosphorylation suppressed by ERα (Fig. 4L), suggesting that the inhibitory effect of ERα on NF-κB be mediated by *LINC00472*.

Suppression of NF-κB phosphorylation by ERα mediated through *LINC00472* was further verified in T47D cells after *LINC00472* expression was suppressed by siRNA (Fig. 5A). Suppressing *LINC00472* expression could increase the phosphorylation of IκBα and p65 while ERα expression was not changed (Fig. 5B). Reducing *LINC00472* expression by siRNA in T47D also increased cell proliferation (Fig. 5C), migration (Fig. 5D) and invasion (Fig. 5E). We also treated T47D cells with tamoxifen for 2 days and 8 days to examine the anti-ER effects on *LINC00472* and NF-κB. As expected, the treatment at both time points lowered the expression of ERα and *LINC00472*, and increased the phosphorylation of IκBα and p65 (Fig. 5F, 5G, and 5H, only the 8-day results shown), further confirming the interactions among ERα, *LINC00472* and NF-κB. Suppressing *LINC00472* expression in human mammary epithelial cells also increased the phosphorylation of IKKβ, IκBα and p65 (Fig. 5I), indicating that the suppression of NF-κB phosphorylation by *LINC00472* occurred in normal cells.

Associations of LINC00472 expression with ER status and patient survival

Of the 11 clinical datasets (our study plus 10 online datasets) with information on ER status and *LINC00472*, 10 showed higher *LINC00472* expression in ER-positive than ER-negative tumors (Fig. 6A). The summarized odds ratio for high *LINC00472* in ER-negative tumors was low, only 0.425 (Fig. 6B). ER-positive patients with high *LINC00472* had better relapse-free survival (Fig. 6C) and overall survival (Fig. 6D) compared to ER-positive patients with low *LINC00472*. The risk for relapse or death was reduced by more than 40% when ER-positive patients had higher *LINC00472*.

Discussion

In this study, we tested *LINC00472* expression in six breast cancer cell lines, all of which had low expression, except T47D. Of these cell lines, three (MCF-7, T47D and ZR-75-1) were ER-positive, but their *LINC00472* expression was quite different. MCF-7 had the lowest expression, while the expression was relatively high in T47D. However, compared to the normal mammary epithelial cells, *LINC00472* expression was low in all the tumor cells. Increasing the expression of *LINC00472* in MCF-7and SKBR3 through transient transfection of a *LINC00472* plasmid could suppress the growth and migration of these cells, suggesting that *LINC00472* may play a role in suppressing breast cancer (13). In order to further evaluate its anti-tumor effects, we stably transfected the *LINC00472* plasmid into two aggressive breast cancer cell lines (MB231 and Hs578T), and the transfection resulted in high expression of *LINC00472* in these cells. Cells with high *LINC00472* expression showed slower growth both *in vitro* and *in vivo*. Furthermore, these cells were less likely to

migrate and invade, and formed fewer colonies. The observations were consistent with the findings of our previous study (13).

To elucidate the molecular targets and regulation, we analyzed the transcription profiles of breast cancer cells overexpressing *LINC00472*, and the analysis indicated a possible effect of the lncRNA on the TNF-α pathway in both cell lines (MB231 and Hs578T). Following the lead, we tested the effect of TNF-α on *LINC00472* expression, and found no direct influence. However, in the experiments, we found that *LINC00472* inhibited the phosphorylation of IκBα and p65, and interacted with one of the NF-κB activating enzymes, IKKβ, suppressing its phosphorylation Our analysis of metabolomes also indicated a possible interaction between *LINC00472* and NF-κB as the lncRNA was predicted to upregulate the degradation of methionine. One study found that methionine restriction inhibited nuclear translocation of NF-κB in tumor cell lines of the central nervous system (22). Another reported that low methionine inhibited the migration and invasion of MB231 and Hs578T cells (23).

Analysis of the transcriptomes of MB231 and Hs578T with *LINC00472* overexpression suggested that *ESR1* be a possible transcription factor for *LINC00472*. An ERα–binding site was also predicted in the *LINC00472* promoter, and the prediction was confirmed by our experiments, showing that ERα was able to bind to the predicted region, upregulating its expression. These results were further supported by our experiments on an ER-positive cell line, T47D, in which *LINC00472* expression was high and suppressing ER by tamoxifen could lower the expression of *LINC00472*. Analysis of multiple online clinical datasets as well as our own study also demonstrated that high expression of *LINC00472* was associated with ER-positive tumors and favorable prognosis in ER-positive patients. Furthermore, our experiments demonstrated that suppression of NF–κB by ERα was mediated through *LINC00472* and that inhibiting *LINC00472* expression in cells could increase the phosphorylation of IKKβ, IκBα and p65. All these findings suggest that *LINC00472* may play an important role in the interaction between NF-κB and ERα which has been implicated in the possible mechanism of endocrine resistance in breast cancer (4).

Some breast cancer patients are resistant or develop resistance to endocrine therapy (3). Several molecular mechanisms have been proposed to explain the phenomenon, one of which is the interaction between ERα and NF-κB (4). Estrogen was found to inhibit inflammation by suppressing the DNA-binding ability of NF-κB (24) or blocking the translocation of NF-κB from cytoplasm to nucleus (25). NF-κB inhibition by estrogen was also observed in a number of studies (26-29). In addition, NF-κB could suppress estrogen (30) and inhibit the activity of ERα (31) or its expression (32). Analysis of tumor samples showed an inverse correlation between ERα and NF-κB in terms of their expression (4, 30, 33, 34). Thus, a reciprocal inhibition was proposed for ERα and NF-κB.

NF-κB is known to be involved in the progression of ER-negative tumors (35-37). In ER-positive tumors, patients with high NF-κB developed resistance to tamoxifen compared to those with low NF-κB (38). Furthermore, ER-positive tumor cells with high NF-κB did not respond well to tamoxifen treatment, and inhibition of NF-κB could reduce tumor resistance to tamoxifen therapy (38-40). Studies also demonstrated that the development of tamoxifen

resistance was accompanied by increased NF-κB activities (41, 42). These observations led to the speculation that ER suppression by endocrine therapy may release NF-κB inhibition, resulting in increased NF-κB activities that promote tumor growth and invasion, leading to disease recurrence and tumor metastasis. In agreement with this speculation, our experiments on T47D showed that tamoxifen treatment of this ER-positive tumor cell line resulted in suppression of *LINC00472*, which led to increased phosphorylation of IκBα and p65.

Our finding of *LINC00472*'s connection to ERα and NF-κB in tumor cells and observations of associations between *LINC00472* expression and ER status and disease outcomes in multiple breast cancer datasets provide new insights into the relationship between ERα and NF-κB and their possible role in endocrine resistance. However, our findings on the link between *LINC00472* expression and ER status was not entirely consistent in cell lines. MCF-7 is ER-positive, but *LINC00472* expression in the cells is quite low compared to T47D. The reason for this difference is not known. There may be other factors, in addition to ER, affecting the expression of *LINC00472*. To test if estrogen affects the expression of *LINC00472*, we treated T47D and MCF-7 with 17β-estradiol (E2) at 100 nM for 0-4 hours. ERα was declined (both mRNA and protein) after the treatment, and *LINC00472* expression was also decreased. The decline of ERα expression after E2 treatment in MCF-7 and T47D has been observed in several other studies (43-45), suggesting the possibility of a negative signal feedback loop in these ER-positive tumor cell lines. Since estrogen metabolism and ER expression are regulated by different mechanisms and ER has estrogen-dependent and independent activities, it is difficult for us to determine the effect of estrogen on ER regulation of *LINC00472* expression in this study. More experiments are needed to address these relationships.

In our analysis of the *LINC00472* transcriptomes, we found an inverse correlation between *LINC00472* and *MALAT1* in tumor cells, but this correlation could not be confirmed in breast cancer patients. We analyzed the expression of *MALAT1* in relation to *LINC00472* in over 300 breast tumor samples, and did not find a significant correlation between these lncRNAs. *MATLAT1* (Metastasis-Associated Lung Adenocarcinoma Transcript 1) is a well-known lncRNA with oncogenic effects on multiple cancer sites (46-49). Our study also showed that high *MALAT1* expression in breast cancer was associated with poor disease-free survival (50).

In summary, increasing *LINC00472* expression in breast tumor cells reduced their aggressive behaviors and suppressed tumor growth. ERα could bind to the *LINC00472* promoter, upregulating its expression. *LINC00472* inhibited the activity of NF-κB and mediated the effect of ERα on suppression of NF-κB phosphorylation. High expression of *LINC00472* was associated with ER-positive breast tumors and favorable survival of ER-positive patients. Tamoxifen treatment of ER-positive tumor cells suppressed *L1NC00472* expression, increasing NF-κB phosphorylation. Taken together, we speculate that long-term use of tamoxifen may reduce the suppression of NF-κB phosphorylation by *LINC00472*, leading to endocrine resistance and tumor progression. Further elucidating the role of *LINC00472* in breast cancer may help to understand the mechanism of endocrine resistance and develop new strategies in breast cancer treatment.

Supplementary Material

Refer to Web version on PubMed Central for supplementary material.

Acknowledgments

Funding: This study was funded by University of Hawaii Cancer Center and Shanghai Jiao Tong University School of Medicine.

References

1. Metzger-Filho O, Sun Z, Viale G, Price KN, Crivellari D, Snyder RD, Gelber RD, Castiglione-Gertsch M, Coates AS, Goldhirsch A, Cardoso F. Patterns of Recurrence and outcome according to breast cancer subtypes in lymph node-negative disease: results from international breast cancer study group trials VIII and IX. Journal of clinical oncology : official journal of the American Society of Clinical Oncology. 2013;31(25):3083–90. Epub 2013/07/31. doi: 10.1200/JCO.2012.46.1574. PubMed PMID: 23897954; PMCID: 3753700. [PubMed: 23897954]
2. Kohler BA, Sherman RL, Howlader N, Jemal A, Ryerson AB, Henry KA, Boscoe FP, Cronin KA, Lake A, Noone AM, Henley SJ, Eheman CR, Anderson RN, Penberthy L. Annual Report to the Nation on the Status of Cancer, 1975-2011, Featuring Incidence of Breast Cancer Subtypes by Race/Ethnicity, Poverty, and State. Journal of the National Cancer Institute. 2015;107(6):djv048. Epub 2015/04/01. doi: 10.1093/jnci/djv048. PubMed PMID: 25825511; PMCID: 4603551. [PubMed: 25825511]
3. Musgrove EA, Sutherland RL. Biological determinants of endocrine resistance in breast cancer. Nature reviews Cancer. 2009;9(9):631–43. Epub 2009/08/25. doi: 10.1038/nrc2713. PubMed PMID: 19701242. [PubMed: 19701242]
4. Sas L, Lardon F, Vermeulen PB, Hauspy J, Van Dam P, Pauwels P, Dirix LY, Van Laere SJ. The interaction between ER and NFkappaB in resistance to endocrine therapy. Breast cancer research : BCR. 2012;14(4):212. Epub 2012/09/12. doi: 10.1186/bcr3196. PubMed PMID: 22963717; PMCID: 3680926. [PubMed: 22963717]
5. Dolcet X, Llobet D, Pallares J, Matias-Guiu X. NF-kB in development and progression of human cancer. Virchows Archiv : an international journal of pathology. 2005;446(5):475–82. Epub 2005/04/28. doi: 10.1007/s00428-005-1264-9. PubMed PMID: 15856292. [PubMed: 15856292]
6. Ben-Neriah Y, Karin M. Inflammation meets cancer, with NF-kappaB as the matchmaker. Nature immunology. 2011;12(8):715–23. Epub 2011/07/21. doi: 10.1038/ni.2060. PubMed PMID: 21772280. [PubMed: 21772280]
7. DiDonato JA, Mercurio F, Karin M. NF-kappaB and the link between inflammation and cancer. Immunological reviews. 2012;246(1):379–400. Epub 2012/03/23. doi: 10.1111/j.1600-065X.2012.01099.x. PubMed PMID: 22435567. [PubMed: 22435567]
8. Rinkenbaugh AL, Baldwin AS. The NF-kappaB Pathway and Cancer Stem Cells. Cells. 2016;5(2). Epub 2016/04/09. doi: 10.3390/cells5020016. PubMed PMID: 27058560; PMCID: 4931665.
9. Wu Y, Deng J, Rychahou PG, Qiu S, Evers BM, Zhou BP. Stabilization of snail by NF-kappaB is required for inflammation-induced cell migration and invasion. Cancer cell. 2009;15(5):416–28. Epub 2009/05/05. doi: 10.1016/j.ccr.2009.03.016. PubMed PMID: 19411070; PMCID: 2881229. [PubMed: 19411070]
10. Djebali S, Davis CA, Merkel A, Dobin A, Lassmann T, Mortazavi A, Tanzer A, Lagarde J, Lin W, Schlesinger F, Xue C, Marinov GK, Khatun J, Williams BA, Zaleski C, Rozowsky J, Roder M, Kokocinski F, Abdelhamid RF, Alioto T, Antoshechkin I, Baer MT, Bar NS, Batut P, Bell K, Bell I, Chakrabortty S, Chen X, Chrast J, Curado J, Derrien T, Drenkow J, Dumais E, Dumais J, Duttagupta R, Falconnet E, Fastuca M, Fejes-Toth K, Ferreira P, Foissac S, Fullwood MJ, Gao H, Gonzalez D, Gordon A, Gunawardena H, Howald C, Jha S, Johnson R, Kapranov P, King B, Kingswood C, Luo OJ, Park E, Persaud K, Preall JB, Ribeca P, Risk B, Robyr D, Sammeth M, Schaffer L, See LH, Shahab A, Skancke J, Suzuki AM, Takahashi H, Tilgner H, Trout D, Walters N, Wang H, Wrobel J, Yu Y, Ruan X, Hayashizaki Y, Harrow J, Gerstein M, Hubbard T, Reymond A, Antonarakis SE, Hannon G, Giddings MC, Ruan Y, Wold B, Carninci P, Guigo R, Gingeras TR.

Landscape of transcription in human cells. Nature. 2012;489(7414):101–8. Epub 2012/09/08. doi: 10.1038/nature11233. PubMed PMID: 22955620; PMCID: 3684276. [PubMed: 22955620]

11. Schmitt AM, Chang HY. Long Noncoding RNAs in Cancer Pathways. Cancer cell. 2016;29(4): 452–63. Epub 2016/04/14. doi: 10.1016/j.ccell.2016.03.010. PubMed PMID: 27070700; PMCID: 4831138. [PubMed: 27070700]
12. Spizzo R, Almeida MI, Colombatti A, Calin GA. Long non-coding RNAs and cancer: a new frontier of translational research? Oncogene. 2012;31(43):4577–87. Epub 2012/01/24. doi: 10.1038/onc.2011.621. PubMed PMID: 22266873; PMCID: 3433647. [PubMed: 22266873]
13. Shen Y, Katsaros D, Loo LW, Hernandez BY, Chong C, Canuto EM, Biglia N, Lu L, Risch H, Chu WM, Yu H. Prognostic and predictive values of long non-coding RNA LINC00472 in breast cancer. Oncotarget. 2015;6(11):8579–92. Epub 2015/04/14. doi: 10.18632/oncotarget.3287. PubMed PMID: 25865225; PMCID: 4496168. [PubMed: 25865225]
14. Shen Y, Wang Z, Loo LW, Ni Y, Jia W, Fei P, Risch HA, Katsaros D, Yu H. LINC00472 expression is regulated by promoter methylation and associated with disease-free survival in patients with grade 2 breast cancer. Breast cancer research and treatment. 2015;154(3):473–82. Epub 2015/11/14. doi: 10.1007/s10549-015-3632-8. PubMed PMID: 26564482; PMCID: 4854534. [PubMed: 26564482]
15. Wang Z, Katsaros D, Shen Y, Fu Y, Canuto EM, Benedetto C, Lu L, Chu WM, Risch HA, Yu H. Biological and Clinical Significance of MAD2L1 and BUB1, Genes Frequently Appearing in Expression Signatures for Breast Cancer Prognosis. PloS one. 2015;10(8):e0136246. Epub 2015/08/20. doi: 10.1371/journal.pone.0136246. PubMed PMID: 26287798; PMCID: 4546117. [PubMed: 26287798]
16. Ni Y, Xie G, Jia W. Metabonomics of human colorectal cancer: new approaches for early diagnosis and biomarker discovery. Journal of proteome research. 2014;13(9):3857–70. Epub 2014/08/12. doi: 10.1021/pr500443c. PubMed PMID: 25105552. [PubMed: 25105552]
17. Qiu Y, Zhou B, Su M, Baxter S, Zheng X, Zhao X, Yen Y, Jia W. Mass spectrometry-based quantitative metabolomics revealed a distinct lipid profile in breast cancer patients. International journal of molecular sciences. 2013;14(4):8047–61. Epub 2013/04/16. doi: 10.3390/ijms14048047. PubMed PMID: 23584023; PMCID: 3645730. [PubMed: 23584023]
18. Qiu Y, Cai G, Zhou B, Li D, Zhao A, Xie G, Li H, Cai S, Xie D, Huang C, Ge W, Zhou Z, Xu LX, Jia W, Zheng S, Yen Y, Jia W. A distinct metabolic signature of human colorectal cancer with prognostic potential. Clinical cancer research : an official journal of the American Association for Cancer Research. 2014;20(8):2136–46. Epub 2014/02/15. doi: 10.1158/1078-0432.CCR-13-1939. PubMed PMID: 24526730. [PubMed: 24526730]
19. Messeguer X, Escudero R, Farre D, Nunez O, Martinez J, Alba MM. PROMO: detection of known transcription regulatory elements using species-tailored searches. Bioinformatics. 2002;18(2):333–4. Epub 2002/02/16. PubMed PMID: 11847087. [PubMed: 11847087]
20. DerSimonian R, Laird N. Meta-analysis in clinical trials. Control Clin Trials. 1986;7(3):177–88. PubMed PMID: 3802833. [PubMed: 3802833]
21. Larsson SC, Giovannucci E, Wolk A. Folate and risk of breast cancer: a meta-analysis. Journal of the National Cancer Institute. 2007;99(1):64–76. doi: 10.1093/jnci/djk006. PubMed PMID: 17202114. [PubMed: 17202114]
22. Kokkinakis DM, Liu X, Chada S, Ahmed MM, Shareef MM, Singha UK, Yang S, Luo J. Modulation of gene expression in human central nervous system tumors under methionine deprivation-induced stress. Cancer research. 2004;64(20):7513–25. doi: 10.1158/0008-5472.CAN-04-0592. PubMed PMID: 15492278. [PubMed: 15492278]
23. Jeon H, Kim JH, Lee E, Jang YJ, Son JE, Kwon JY, Lim TG, Kim S, Park JH, Kim JE, Lee KW. Methionine deprivation suppresses triple-negative breast cancer metastasis in vitro and in vivo. Oncotarget. 2016;7(41):67223–34. doi: 10.18632/oncotarget.11615. PubMed PMID: 27579534; PMCID: PMC5341870. [PubMed: 27579534]
24. Paimela T, Ryhanen T, Mannermaa E, Ojala J, Kalesnykas G, Salminen A, Kaarniranta K. The effect of 17beta-estradiol on IL-6 secretion and NF-kappaB DNA-binding activity in human retinal pigment epithelial cells. Immunology letters. 2007;110(2):139–44. Epub 2007/05/29. doi: 10.1016/j.imlet.2007.04.008. PubMed PMID: 17532054. [PubMed: 17532054]

25. Ghisletti S, Meda C, Maggi A, Vegeto E. 17beta-estradiol inhibits inflammatory gene expression by controlling NF-kappaB intracellular localization. Molecular and cellular biology. 2005;25(8): 2957–68. Epub 2005/03/31. doi: 10.1128/MCB.25.8.2957-2968.2005. PubMed PMID: 15798185; PMCID: 1069609. [PubMed: 15798185]
26. Galien R, Garcia T. Estrogen receptor impairs interleukin-6 expression by preventing protein binding on the NF-kappaB site. Nucleic acids research. 1997;25(12):2424–9. Epub 1997/06/15. PubMed PMID: 9171095; PMCID: 146754. [PubMed: 9171095]
27. Nettles KW, Gil G, Nowak J, Metivier R, Sharma VB, Greene GL. CBP Is a dosage-dependent regulator of nuclear factor-kappaB suppression by the estrogen receptor. Molecular endocrinology. 2008;22(2):263–72. Epub 2007/10/13. doi: 10.1210/me.2007-0324. PubMed PMID: 17932106; PMCID: 2234588. [PubMed: 17932106]
28. Hsu SM, Chen YC, Jiang MC. 17 beta-estradiol inhibits tumor necrosis factor-alpha-induced nuclear factor-kappa B activation by increasing nuclear factor-kappa B p105 level in MCF-7 breast cancer cells. Biochemical and biophysical research communications. 2000;279(1):47–52. Epub 2000/12/09. doi: 10.1006/bbrc.2000.3891. PubMed PMID: 11112416. [PubMed: 11112416]
29. Wang X, Belguise K, Kersual N, Kirsch KH, Mineva ND, Galtier F, Chalbos D, Sonenshein GE. Oestrogen signalling inhibits invasive phenotype by repressing RelB and its target BCL2. Nature cell biology. 2007;9(4):470–8. Epub 2007/03/21. doi: 10.1038/ncb1559. PubMed PMID: 17369819; PMCID: 2394707. [PubMed: 17369819]
30. Van Laere SJ, Van der Auwera I, Van den Eynden GG, van Dam P, Van Marck EA, Vermeulen PB, Dirix LY. NF-kappaB activation in inflammatory breast cancer is associated with oestrogen receptor downregulation, secondary to EGFR and/or ErbB2 overexpression and MAPK hyperactivation. British journal of cancer. 2007;97(5):659–69. Epub 2007/08/19. doi: 10.1038/sj.bjc.6603906. PubMed PMID: 17700572; PMCID: 2360371. [PubMed: 17700572]
31. Qiu J, Wang X, Guo X, Zhao C, Wu X, Zhang Y. Toll-like receptor 9 agonist inhibits ERalpha-mediated transactivation by activating NF-kappaB in breast cancer cell lines. Oncology reports. 2009;22(4):935–41. Epub 2009/09/03. PubMed PMID: 19724876. [PubMed: 19724876]
32. Wang X, Belguise K, O'Neill CF, Sanchez-Morgan N, Romagnoli M, Eddy SF, Mineva ND, Yu Z, Min C, Trinkaus-Randall V, Chalbos D, Sonenshein GE. RelB NF-kappaB represses estrogen receptor alpha expression via induction of the zinc finger protein Blimp1. Molecular and cellular biology. 2009;29(14):3832–44. Epub 2009/05/13. doi: 10.1128/MCB.00032-09. PubMed PMID: 19433448; PMCID: 2704748. [PubMed: 19433448]
33. Van Laere SJ, Van der Auwera I, Van den Eynden GG, Elst HJ, Weyler J, Harris AL, van Dam P, Van Marck EA, Vermeulen PB, Dirix LY. Nuclear factor-kappaB signature of inflammatory breast cancer by cDNA microarray validated by quantitative real-time reverse transcription-PCR, immunohistochemistry, and nuclear factor-kappaB DNA-binding. Clinical cancer research : an official journal of the American Association for Cancer Research. 2006;12(11 Pt 1):3249–56. Epub 2006/06/03. doi: 10.1158/1078-0432.CCR-05-2800. PubMed PMID: 16740744. [PubMed: 16740744]
34. Parker JS, Mullins M, Cheang MC, Leung S, Voduc D, Vickery T, Davies S, Fauron C, He X, Hu Z, Quackenbush JF, Stijleman IJ, Palazzo J, Marron JS, Nobel AB, Mardis E, Nielsen TO, Ellis MJ, Perou CM, Bernard PS. Supervised risk predictor of breast cancer based on intrinsic subtypes. Journal of clinical oncology : official journal of the American Society of Clinical Oncology. 2009;27(8):1160–7. Epub 2009/02/11. doi: 10.1200/JCO.2008.18.1370. PubMed PMID: 19204204; PMCID: 2667820. [PubMed: 19204204]
35. Nakshatri H, Bhat-Nakshatri P, Martin DA, Goulet RJ Jr., Sledge GW Jr. Constitutive activation of NF-kappaB during progression of breast cancer to hormone-independent growth. Molecular and cellular biology. 1997;17(7):3629–39. Epub 1997/07/01. PubMed PMID: 9199297; PMCID: 232215. [PubMed: 9199297]
36. Sovak MA, Bellas RE, Kim DW, Zanieski GJ, Rogers AE, Traish AM, Sonenshein GE. Aberrant nuclear factor-kappaB/Rel expression and the pathogenesis of breast cancer. The Journal of clinical investigation. 1997;100(12):2952–60. Epub 1998/01/31. doi: 10.1172/JCI119848. PubMed PMID: 9399940; PMCID: 508506. [PubMed: 9399940]

37. Cao Y, Karin M. NF-kappaB in mammary gland development and breast cancer. Journal of mammary gland biology and neoplasia. 2003;8(2):215–23. Epub 2003/11/26. PubMed PMID: 14635796. [PubMed: 14635796]
38. Zhou Y, Eppenberger-Castori S, Marx C, Yau C, Scott GK, Eppenberger U, Benz CC. Activation of nuclear factor-kappaB (NFkappaB) identifies a high-risk subset of hormone-dependent breast cancers. The international journal of biochemistry & cell biology. 2005;37(5):1130–44. Epub 2005/03/04. doi: 10.1016/j.biocel.2004.09.006. PubMed PMID: 15743683. [PubMed: 15743683]
39. Riggins RB, Zwart A, Nehra R, Clarke R. The nuclear factor kappa B inhibitor parthenolide restores ICI 182,780 (Faslodex; fulvestrant)-induced apoptosis in antiestrogen-resistant breast cancer cells. Molecular cancer therapeutics. 2005;4(1):33–41. Epub 2005/01/20. PubMed PMID: 15657351. [PubMed: 15657351]
40. deGraffenried LA, Chandrasekar B, Friedrichs WE, Donzis E, Silva J, Hidalgo M, Freeman JW, Weiss GR. NF-kappa B inhibition markedly enhances sensitivity of resistant breast cancer tumor cells to tamoxifen. Annals of oncology : official journal of the European Society for Medical Oncology. 2004;15(6):885–90. Epub 2004/05/21. PubMed PMID: 15151944. [PubMed: 15151944]
41. Kim MR, Choi HK, Cho KB, Kim HS, Kang KW. Involvement of Pin1 induction in epithelial-mesenchymal transition of tamoxifen-resistant breast cancer cells. Cancer science. 2009;100(10): 1834–41 Epub 2009/08/18. doi: 10.1111/j.1349-7006.2009.01260.x. PubMed PMID: 19681904. [PubMed: 19681904]
42. Zhou Y, Yau C, Gray JW, Chew K, Dairkee SH, Moore DH, Eppenberger U, Eppenberger-Castori S, Benz CC. Enhanced NF kappa B and AP-1 transcriptional activity associated with antiestrogen resistant breast cancer. BMC cancer. 2007;7:59. Epub 2007/04/05. doi: 10.1186/1471-2407-7-59. PubMed PMID: 17407600; PMCID: 1852565. [PubMed: 17407600]
43. La Rosa P, Pellegrini M, Totta P, Acconcia F, Marino M. Xenoestrogens alter estrogen receptor (ER) alpha intracellular levels. PloS one. 2014;9(2):e88961. doi: 10.1371/journal.pone.0088961. PubMed PMID: 24586459; PMCID: PMC3930606. [PubMed: 24586459]
44. Zhang Y, Zhao H, Asztalos S, Chisamore M, Sitabkhan Y, Tonetti DA. Estradiol-induced regression in T47D:A18/PKCalpha tumors requires the estrogen receptor and interaction with the extracellular matrix. Mol Cancer Res. 2009;7(4):498–510. doi: 10.1158/1541-7786.MCR-08-0415. PubMed PMID: 19372579; PMCID: PMC2743931. [PubMed: 19372579]
45. Long X, Fan M, Bigsby RM, Nephew KP. Apigenin inhibits antiestrogen-resistant breast cancer cell growth through estrogen receptor-alpha-dependent and estrogen receptor-alpha-independent mechanisms. Molecular cancer therapeutics. 2008;7(7):2096–108. doi: 10.1158/1535-7163.MCT-07-2350. PubMed PMID: 18645020; PMCID: PMC2559959. [PubMed: 18645020]
46. Zhou X, Liu S, Cai G, Kong L, Zhang T, Ren Y, Wu Y, Mei M, Zhang L, Wang X. Long Non Coding RNA MALAT1 Promotes Tumor Growth and Metastasis by inducing Epithelial-Mesenchymal Transition in Oral Squamous Cell Carcinoma. Sci Rep. 2015;5:15972. doi: 10.1038/srep15972. PubMed PMID: 26522444; PMCID: PMC4629155. [PubMed: 26522444]
47. Taheri M, Omrani MD, Ghafouri-Fard S. Long non-coding RNA expression in bladder cancer. Biophys Rev. 2017. doi: 10.1007/s12551-017-0379-y. PubMed PMID: 29222807.
48. Zhang X, Hamblin MH, Yin KJ. The long noncoding RNA Malat1: Its physiological and pathophysiological functions. RNA Biol. 2017;14(12):1705–14. doi: 10.1080/15476286.2017.1358347. PubMed PMID: 28837398; PMCID: PMC5731810. [PubMed: 28837398]
49. Yoshimoto R, Mayeda A, Yoshida M, Nakagawa S. MALAT1 long non-coding RNA in cancer. Biochim Biophys Acta. 2016;1859(1):192–9. doi: 10.1016/j.bbagrm.2015.09.012. PubMed PMID: 26434412. [PubMed: 26434412]
50. Wang Z, Katsaros D, Biglia N, Shen Y, Fu Y, Loo LWM, Jia W, Obata Y, Yu H. High expression of long non-coding RNA MALAT1 in breast cancer is associated with poor relapse-free survival. Breast cancer research and treatment. 2018. doi: 10.1007/s10549-018-4839-2. PubMed PMID: 29845475.

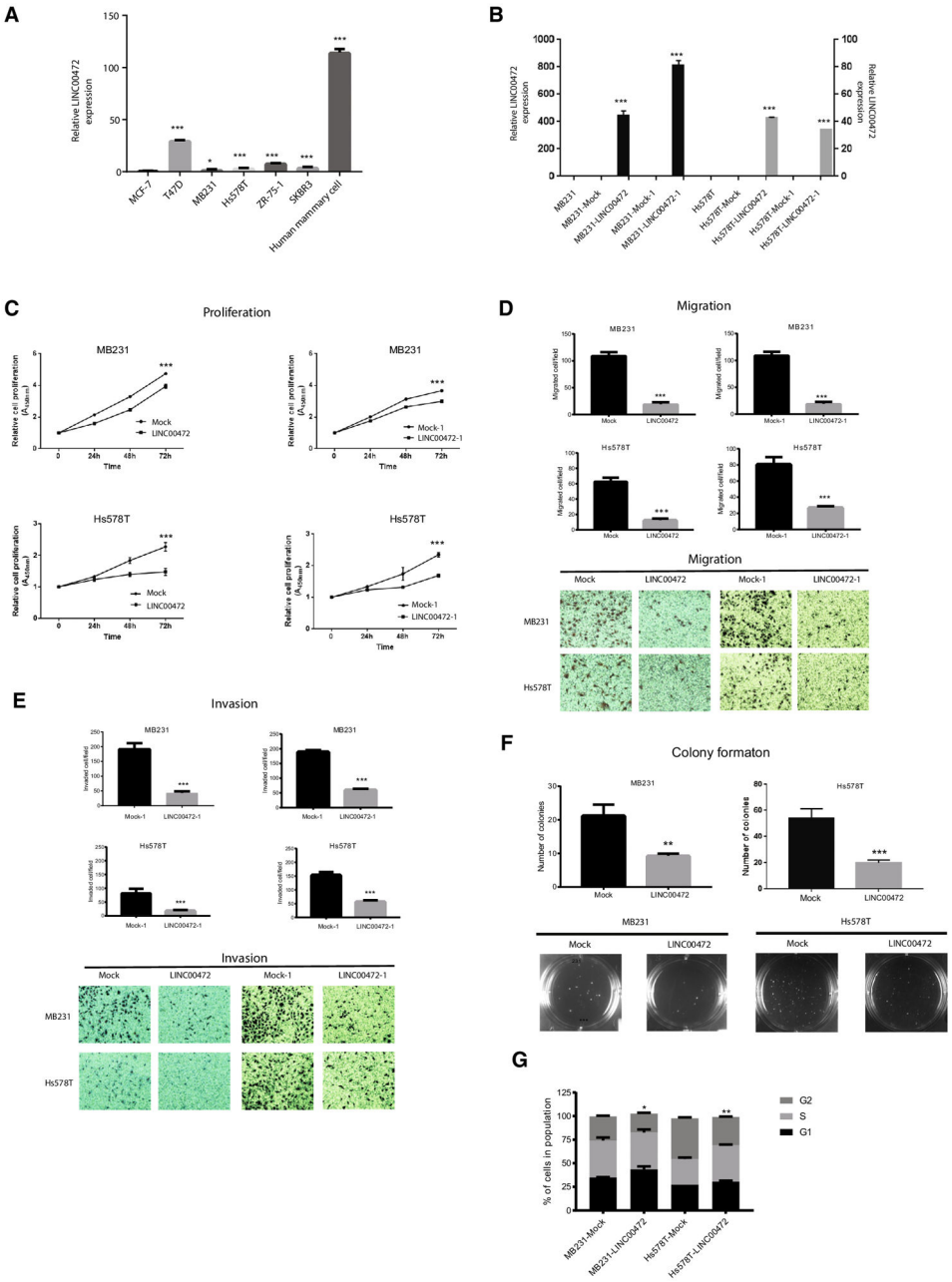

Figure 1. *LINC00472* expression in breast cell lines and suppression of tumor cell proliferation, migration, invasion, and colony formation by *LINC00472*.

A. *LINC00472* expression was low in all the breast cancer cell lines tested, except T47D. Human primary mammary epithelial cells had the highest expression of *LINC00472*. Comparisons were made between MCF-7 and other cell lines. *=P<0.05, ***=P<0.0001.

B. *LINC00472* expression was significantly increased in MB231 and Hs578T cells transfected with a *LINC00472*-expressing plasmid (pool: MB231-LINC00472 and Hs578T-LINC00472; single clone: MB231-LINC00472-1 and Hs578T-LINC00472-1), in comparison to those transfected with an empty vector (mock) (pool: MB231-Mock and Hs578T-Mock; single clone: MB231-Mock-1 and Hs578T-Mock-1). β-actin was used as

reference in expression analysis. Comparisons were made between cells transfected with a *LINC00472* plasmid and mock plasmid. ***=P<0.0001.

C. Cell proliferation assay showed that MB231 and Hs578T cells with *LINC00472* overexpression grew slower than those without overexpression. ***=P<0.0001.

D. Cell migration assay showed that fewer MB231 and Hs578T cells with *LINC00472* overexpression migrated compared to those without overexpression. ***=P<0.0001.

E. Cell invasion assay showed that fewer MB231 and Hs578T cells with *LINC00472* overexpression invaded compared to those without overexpression. ***=P<0.0001.

F. Colony formation assay showed that fewer colonies were formed in MB231 and Hs578T cells with *LINC00472* overexpression compared to those without overexpression. **=P<0.001, ***=P<0.0001.

G. Flow cytometry analysis of cell cycle showed that fewer MB231 and Hs578T cells with *LINC00472* overexpression were in G_2 phase compared to those without overexpression. *=P<0.05, ***=P<0.0001.

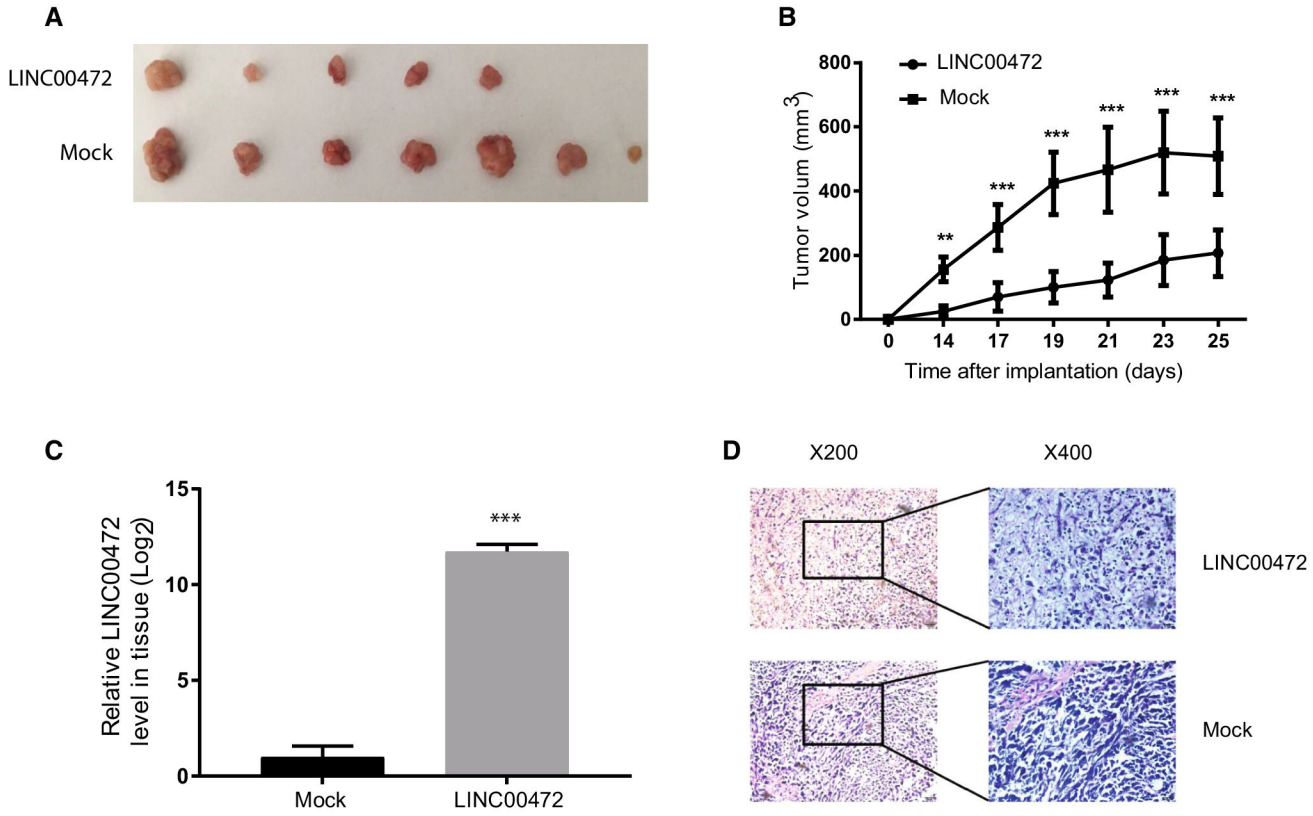

Figure 2. Inhibition of breast tumor growth by *LINC00472* in a xenograft mouse model.

A. Seven BALB/c female nude mice received mammary fat pad injection of MB231cells. Cells with *LINC00472* overexpression were on the left side and those without overexpression were on the right. Seven pairs of tumors dissected from the left (top line) and right (bottom line) mammary fat pad after 25 weeks of injection were displayed. Tumors on the top were smaller than those on the bottom. No tumors were detected in the left fat pad of two mice.

B. Average tumor volumes (mm^3) measured at each time post injection (days) were significantly smaller in the side with *LINC00472* overexpression cells (left) than the side without overexpression (right). ***=P<0.0001.

C. *LINC00472* levels in tumor samples were much higher in the side with *LINC00472* overexpression (left) than the side without overexpression (right). ***=P<0.0001.

D. H&E staining of tumor tissues showed that tumors with *LINC00472* overexpression had fewer cells and less malignant morphology than those without overexpression.

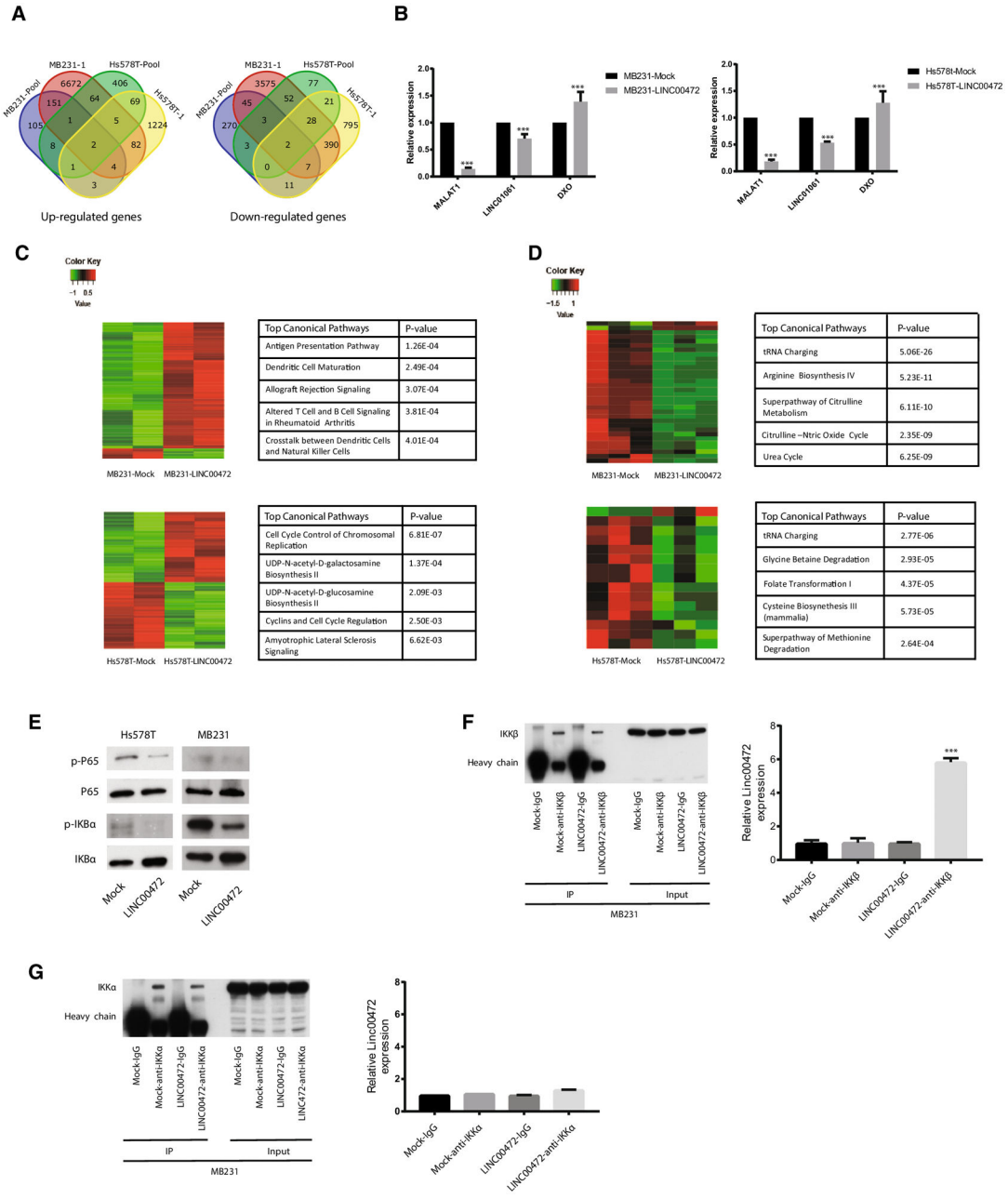

Figure 3. Analysis of transcriptome and metabolome and suppression of p65 and IκBα phosphorylation by *LINC00472*.

A. Venn diagram showed the number of genes up- and down-regulated in MB231 and Hs578T cells due to *LINC00472* overexpression (two pools and two single clones in each cell line, a total 8 samples in 4 strips in the up- and down-regulated expression panels).

B. Expression of one up- (*DXO*) and two down-regulated (*LINC01061*, *MALAT1*) genes measured by qRT-PCR in MB231 (3B left) and Hs578T (3B right). Sequences of the PCR primers are shown in Supplementary Table 2. ***=P<0.0001.

C. Heatmap showed differentially expressed genes in MB231 and Hs578T cells due to *LINC00472* overexpression; top five canonical pathways were predicted by Ingenuity

Pathway Analysis (IPA) based on the differentially expressed genes (2-fold change in expression due to *LINC00472* overexpression and $p<0.05$) in MB231 and Hs578T.

D. Heatmap showed differentially detected metabolites in MB231 and Hs578T cells due to *LINC00472* overexpression; top five canonical pathways were predicted by IPA based on the differentially detected metabolites in MB231 and Hs578T.

E. Western blot analysis showed reduced phosphorylation of p65 (p-P65) and IκBα (p-IκBα in MB231 and Hs578T cells with *LINC00472* overexpression.

F. RIP assay results indicated the binding of IKKβ to *LINC00472*. ***=$P<0.0001$.

G. RIP assay results indicated no binding between IKKα and *LINC00472*.

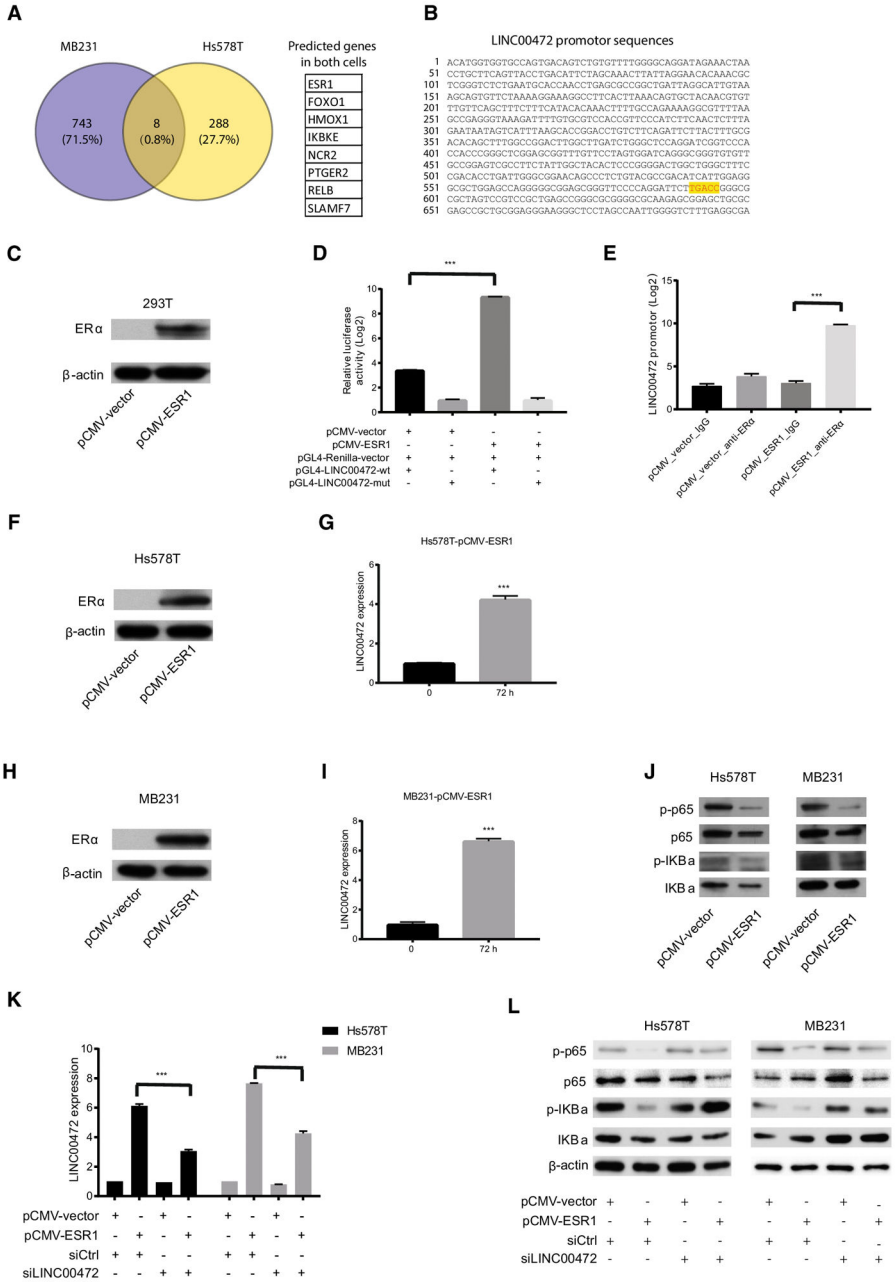

Figure 4. Upregulation of *LINC00472* expression by ERα and ERα-suppressed phosphorylation of p65 and IκBα mediated by *LINC00472*.

A. IPA predicted 743 and 288 possible upstream signals for *LINC00472* in MB231 and Hs578T, respectively. Among these genes, 8, including *ESR1*, *FOXO1*, *HMOX1*, *IKBKE*, *NCR2*, *PTGER2*, *RELB and SLAMF7*, were shared in both cell lines.

B. PROMO predicted an ERα binding site in the *LINC00472* promoter between −591 and −595.

C. Western blot analysis showed increased ERα expression in 293T cells after an *ESR1*-expressing plasmid (pCMV-ESR1) was transfected into the cells.

D. Luciferase reporter assay showed an interaction between ERα and the *LINC00472* promoter predicted by PROMO (Figure 4B) in 293T after the cells were co-transfected with the *ESR1* plasmid (pCMV-ESR1) and a luciferase report, linked either to a wild type of *LINC00472* promoter (pGL4-LINC00472-wt) or a mutant (pGL4-LINC00472-mut).
E. ChIP-qPCR analysis showed an interaction between ERα and the *LINC00472* promoter in 293T transfected with pCMV-ESR1 compared to 293T transfected with pCMV-vector. ***=P<0.0001.
F. Western blot analysis showed increased ERα expression in Hs578T after the cells were transfected with the *ESR1* plasmid (pCMV-ESR1).
G. qRT-PCR analysis showed increased *LINC00472* expression after 72-hour incubation of Hs578T cells with ERα overexpression. ***=P<0.0001.
H. Western blot analysis showed increased ERα expression in MB231 after the cells were transfected with the *ESR1* plasmid (pCMV-ESR1).
I. qRT-PCR analysis showed increased *LINC00472* expression after 72-hour incubation of MB231 cells with ERα overexpression. ***=P<0.0001.
J. Western blot analysis showed suppression of p65 (p-p65) and IκBα (p-IκBα) phosphorylation by ERα in Hs578T and MB231 after the cells were transfected with the *ESR1* plasmid (pCMV-ESR1).
K. qRT-PCR analysis showed significant reduction of *LINC00472* expression in Hs578T and MB231 after knockdown *LINC00472* by siRNA (siLINC00472). ***=P<0.0001.
L. Western blot analysis showed reduced phosphorylation of p65 and IκBα by ERα overexpression in Hs578T and MB231, and increased phosphorylation of p65 and IκBα when *LINC00472* expression in these cells was inhibited by siRNA, suggesting that *LINC00472* may mediate the effect of ERα on suppression of NF-κB.

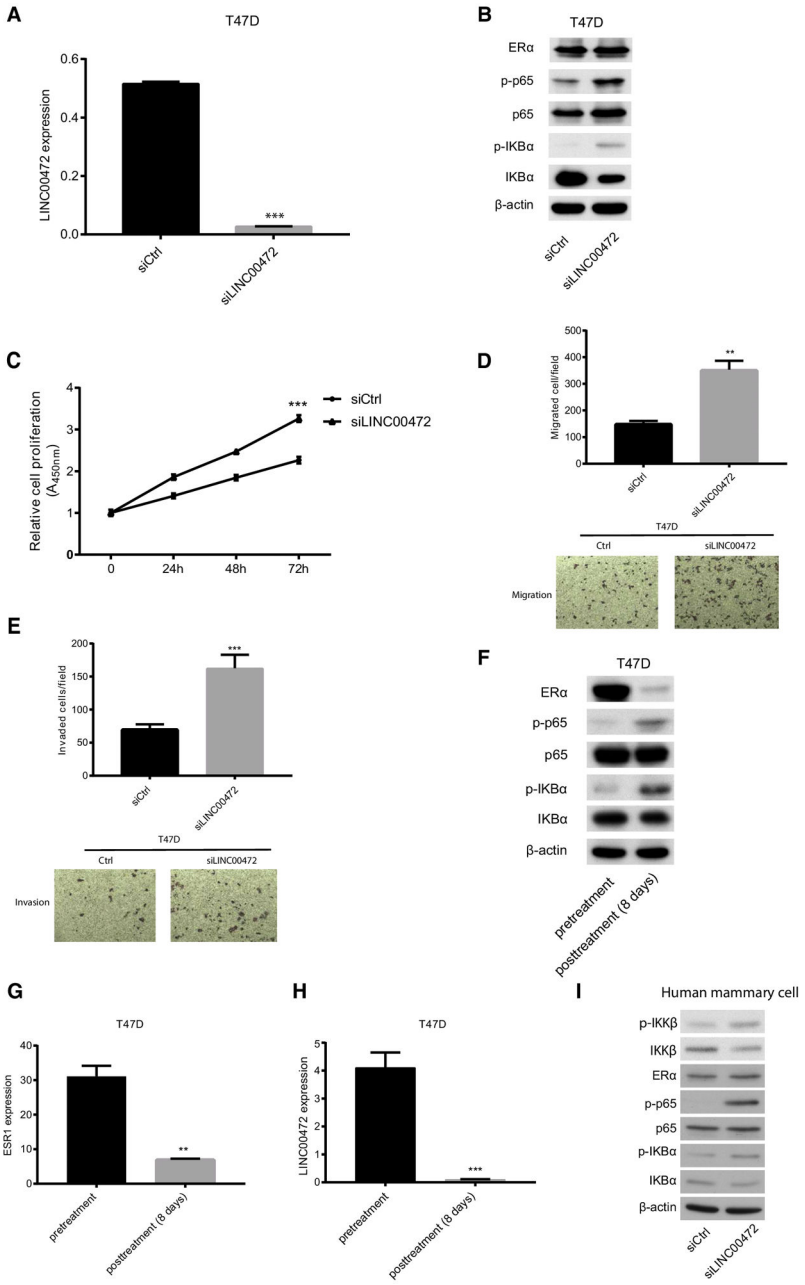

Figure 5. Increased p65 and IκBα phosphorylation, cell proliferation, migration, and invasion after *LINC00472* suppression by siRNA or tamoxifen treatment of T47D cells.

A. qRT-PCR analysis showed reduced *LINC00472* expression in T47D after treatment of *LINC00472* siRNA (siLINC00472). ***=P<0.0001.

B. Western blot analysis showed increased phosphorylation of p65 and IκBα and no change in ERα in T47D after treatment of *LINC00472* siRNA (siLINC00472).

C. Cell proliferation assay showed increased T47D growth after treatment of *LINC00472* siRNA (siLINC00472) compared to control siRNA (siCtrl).

D. Cell migration assay showed increased T47D migration after treatment of *LINC00472* siRNA (siLINC00472) compared to control siRNA (siCtrl).

E. Cell invasion assay showed increased T47D invasion after treatment of *LINC00472* siRNA (siLINC00472) compared to control siRNA (siCtrl).
F. Western blot analysis showed increased phosphorylation of p65 and IκBα and decreased expression of ERα in T47D cells after treatment of 4-hydroxytamoxifen for 8 days.
G. qRT-PCR analysis showed decreased expression of ESR1 in T47D cells after treatment of the cells with 4-hydroxytamoxifen for 8 days. **=P<0.001
H. qRT-PCR analysis showed decreased expression of *LINC00472* in T47D cells after treatment of the cells with 4-hydroxytamoxifen for 8 days. ***=P<0.0001.
I. Western blot analysis showed increased phosphorylation of p65, IκBα and IKKβ in human mammary epithelial cells after *LINC00472* expression was suppressed by siRNA.

A

Dataset	Sample Size	LINC00472				P value
		ER Positive		ER Negative		
		Mean	SD	Mean	SD	
GSE42568	101	1.54	0.46	1.30	0.15	0.0003
GSE53031	167	1.99	0.23	1.91	0.18	0.0204
GSE7390	198	2.75	0.35	2.60	0.44	0.0176
GSE22219	216	2.79	0.06	2.78	0.04	0.0216
GSE4922	245	2.36	0.23	2.27	0.23	0.0408
GSE3494	247	2.36	0.23	2.27	0.23	0.0392
GSE21653	263	1.86	0.34	1.66	0.27	<.0001
GSE2034	286	6.09	1.11	5.54	1.09	0.0003
GSE31448	350	1.81	0.33	1.68	0.28	<.0001
GSE25066	502	2.79	0.37	2.79	0.35	0.8343
Our study	513	5.15	1.68	4.04	1.67	<.0001

B

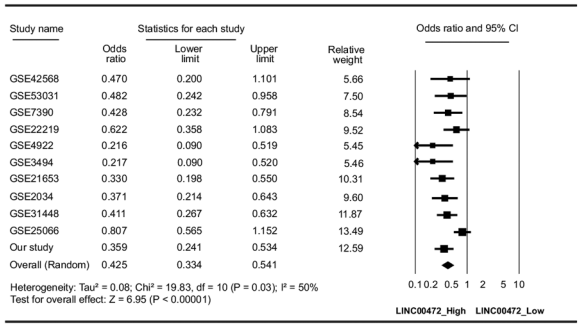

C

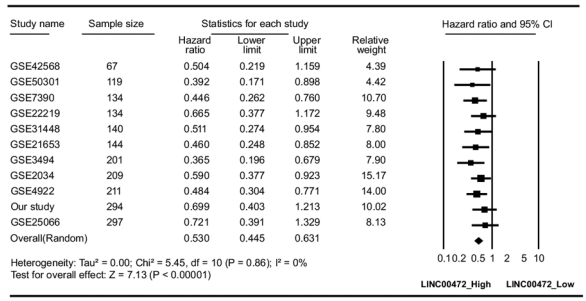

D

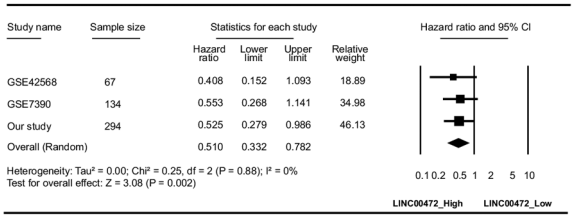

Figure 6. Associations of *LINC00472* expression with ER status and breast cancer survival in patients with ER-positive tumors.

A. Levels of *LINC00472* expression by ER status in our study and 10 online datasets. *LINC00472* expression was significantly higher ($p<0.05$) in ER-positive than ER-negative tumors in 9 of the 10 datasets.

B. Meta-analysis of the association between *LINC00472* expression and ER status. High *LINC00472* expression was less likely to be in ER-negative tumors (summarized odds ratio = 0.425, 95%CI 0.334-0.541).

C. Meta-analysis of the association between *LINC00472* expression and disease-free survival in patients with ER-positive breast cancer. High *LINC00472* expression was

associated with reduced risk of relapse (summarized hazards ratio for relapse was 0.530, 95%CI 0.445-0.631).

D. Meta-analysis of the association between *LINC00472* expression and overall survival in patients with ER-positive breast cancer. High *LINC00472* expression was associated with reduced risk of death (summarized hazards ratio for death was 0.510, 95%CI: 0.332-0.782).